



Synthesis, X-ray diffraction analysis, and chemical–optical characterizations of boron complexes from bidentate ligands

Mario Rodríguez^a, José Luis Maldonado^{a,*}, Gabriel Ramos-Ortíz^a, Oscar Domínguez^b, Ma. Eugenia Ochoa^b, Rosa Santillan^{b,*}, Norberto Farfán^c, Marco-Antonio Meneses-Nava^a, Oracio Barbosa-García^a

^aCentro de Investigaciones en Óptica, Apdo. Postal 1-948, 37000 León, Gto., Mexico

^bDepto. de Química, Centro de Investigación y de Estudios Avanzados del IPN, Apdo. Postal 14-740, 07000 México, D.F., Mexico

^cFacultad de Química, Depto. de Química Orgánica, Universidad Nacional Autónoma de México, 04510 México, D.F., Mexico

ARTICLE INFO

Article history:

Received 17 February 2012

Accepted 19 June 2012

Available online 26 June 2012

Keywords:

Borinates

X-ray analysis

Cubic NLO properties

THG Maker-Fringes technique

ABSTRACT

Herein is reported the synthesis and X-ray diffraction analysis for three boron complexes (**2a–2c**) prepared from the reaction of bidentate ligands (**1a–1c**) and diphenylborinic acid. Chemical characterization for the borinates is completed with IR, UV–Vis and NMR techniques, particularly ¹¹B NMR spectra confirmed the formation of boron complexes. X-ray diffraction analysis showed that for compounds **2a** and **2c** a non-planar conformation for the main π -backbone is acquired after boron complexation; for compound **2b** the planar conformation is preserved. Additionally, cubic nonlinear optical (NLO) properties were evaluated, through the optical susceptibility $\chi^{(3)}$ (-3ω , ω , ω , ω), using the THG Maker-Fringes technique. Results showed that $\chi^{(3)}$ response decreases from ligands to boron complexes; this behavior could be attributed to a structural conformation or deformation of the electronic π -system after boron complexation. The demonstrated electronic and structural features of these borinates could be useful for new strategies in the design of novel NLO dyes.

© 2012 Elsevier Ltd. All rights reserved.

1. Introduction

Comprehension of the structural and electronic properties of organic boron compounds containing the N \rightarrow B coordinative bond have let their use in different fields of applications such as in supramolecular chemistry [1], as a labeled of biological molecules [2], and as sensors [3]. For those compounds having a π -conjugated system, they have also been used as optoelectronic materials with applications in light-emitting diodes (OLEDs) [4], photorefractive (PR) polymers [5], and as dopants of liquid crystals [6]. In particular, the N \rightarrow B bond results interesting when the “*p*” orbital of the boron atom is involved with the non-bonding electron pair of the nitrogen producing a dative bond or a donor–acceptor complex [7]. For instance, the electronic characteristics promoted for this bond on π -systems have been employed to tune the luminescent properties of organic materials [8]. Very recently, for some interesting four-coordinate boron complexes, their luminescent properties were also reported [9].

With respect to the search for novel organic and organometallic compounds with linear and nonlinear optical responses, there is an extensive investigation [10–12]. Nonlinear optical (NLO) behavior

arises from the interaction of an intense electromagnetic field with matter that produces new field components, which could differ in frequency, amplitude, phase, path, polarization, etc. These NLO properties are of enormous technological importance for optical devices with applications in data storage, communication, switching, image processing, and computing. Organic and organometallic materials are attractive for these applications because in many cases they exhibit exceptional NLO features, and in addition, satisfactory mechanical and structural properties (processing, stability, etc.). In particular, considerable efforts to develop materials with third-order nonlinear properties have focused on conjugated organic–organometallic molecules and polymers, containing donor (D) and acceptor (A) groups bridged by a π -electronic system in different arrangements [13–15]; one of the most efficient and widely study structure is precisely the D– π –A one [14,15]. Cubic NLO response is governed at the macroscopic level by the third order susceptibility $\chi^{(3)}$ and offers a more varied and richer behavior than second-order NLO processes due to higher dimensionality of the frequency space [12,16]. Some molecular characteristics have been identified to increase $\chi^{(3)}$ as the conjugation length, heteroaromatic conjugation, degree of strength of the D/A substituents, and the molecular asymmetry [15–18].

We have previously reported the NLO properties of some series of ligands and boron complexes containing the coordinative N \rightarrow B bond on electronic *push–pull* systems [19–21]. These compounds

* Corresponding authors. Tel.: +52 477 441 4200; fax: +52 477 441 4209.

E-mail addresses: jlmr@cio.mx (J.L. Maldonado), rsantill@cinvestav.mx (R. Santillan).

show $\chi^{(3)}$ values between 1.1 and 11×10^{-12} esu at infrared laser wavelengths. Some optical applications of these ligands and boron compounds have been demonstrated by our group and others, they include switch properties [22], photorefractive polymers [5,23,24], and photovoltaic devices (OPVs cells) [25,26]. In this work, the synthesis of the ligands **1b–1c** was carried out for a better understanding of the effect on the chemical–optical features due to the planarity and electronic properties modifications, promoted for the coordinated N → B bond on the aza- π -backbone. We report the chemical characterization for the boron complexes **2b–2c**; their structures, including those for ligands **1b–1c** and the very recently reported borinate **2a** [9], were confirmed by X-ray diffraction analysis. NLO properties for these ligands and their borinates, particularly the cubic susceptibility $\chi^{(3)}$, were also investigated.

2. Experimental

2.1. Materials and methods

All starting materials were purchased from Aldrich Chemical Co. Solvents were used without further purification. ^1H and ^{13}C NMR data of borinate **2a** were compared with the information found in the cited Ref. [9]. Melting points were obtained with an electrothermal 9200 apparatus and are uncorrected. Infrared spectra were measured on a FT-IR spectrometer Spectrum RX1 Perkin–Elmer using attenuated total reflection (ATR). ^1H , ^{13}C and ^{11}B NMR spectra were recorded on Jeol ECA +500 and Bruker Advance DPX 300 spectrometers. Chemical shifts (ppm) are relative to $(\text{CH}_3)_4\text{Si}$ for ^1H and ^{13}C and $\text{BF}_3 \cdot \text{Et}_2\text{O}$ for ^{11}B .

2.2. Synthesis

The ligands **1a–1c** (see Scheme 1) were obtained from classical imine formation reaction, through condensation of the corresponding aldehyde and amine in methanol as a solvent at reflux temperature using a Dean–Stark trap for removing the water obtained during the reaction [27]. Compounds **1a** and **1b** have a strong electron donor (Et_2N) group and acceptor (NO_2) group connected to the conjugated electronic π -backbone for the generation of a “push–pull” architecture on these molecules. Furthermore, the combination of salicylaldehyde–aniline or benzaldehyde–aminophenol in **1a–1b** promotes the formation of six or five boron heterocycle members after boron complexation, respectively. Compounds **2a–2c** were prepared from the equimolar reactions of their corresponding ligands **1a–1c** with freshly liberated diphenylborinic acid

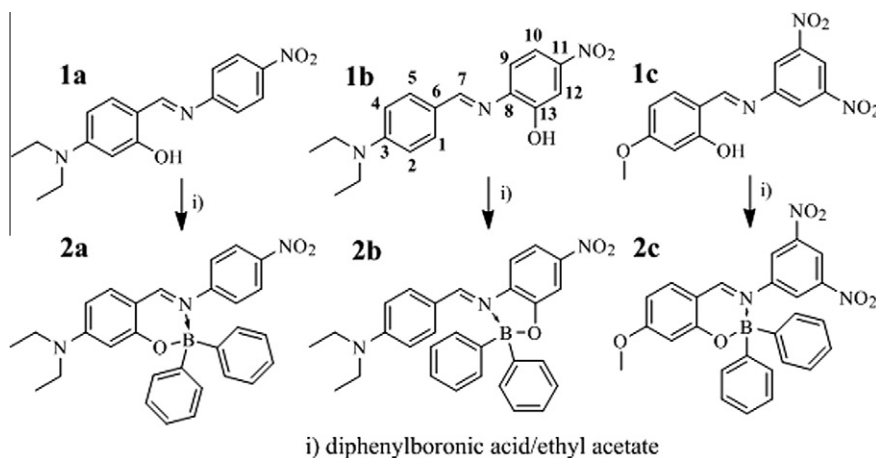
obtained by hydrolysis of the ethanolamine ester complex [28]. Formation of the boron compounds was confirmed through IR, ^1H , ^{13}C and ^{11}B NMR techniques. Evidence for the creation of borinates was obtained from the signal of the tetra-coordinated boron atom at 5.4 ppm for **2a** [9], 11.6 ppm for **2b** and 6.0 ppm for **2c** in the ^{11}B NMR spectra [19].

2.2.1. **2b**: *N,N*-Diethyl-4-((2,2-diphenyl-6-nitrobenzo[d][1,3,2]oxazaborol-3(2H)-ylidene)methyl)benzenamine

The title compound was prepared from the reaction of ligand **1b** 0.85 g (2.7 mmol) and diphenylborinic acid 0.51 g (2.8 mmol) in ethyl ether as a solvent at reflux temperature for 2 h to give 0.95 g (2.1 mmol, 74% yield). MP 198–200 °C. IR ν_{max} (ATR): 2986, 1607, 1598, 1513, 1403, 1327, 1274, 1197, 1152, 1069, 875, 742, 704 cm^{-1} . ^1H NMR (CDCl_3 , 300 MHz) δ : 1.14 (6H, t, $J = 6.9$ Hz, CH_3), 3.50 (4H, q, $J = 6.9$ Hz, N- CH_2), 6.36 (2H, d, $J = 9$ Hz, H-1), 7.24–7.18 (6H, m, H- m,m',p,p'), 7.46 (1H, d, $J = 8.7$ Hz, H-9), 7.54 (4H, d, $J = 6.6$ Hz, H- o,o'), 7.62 (1H, d, $J = 9$ Hz, H-1), 7.64 (1H, s, H-12), 7.70 (1H, d, $J = 8.7$ Hz, H-10), 8.58 (1H, s, H-7) ppm. ^{13}C NMR (CDCl_3 , 75 MHz) δ : 12.4 (CH_3), 44.9 (N- CH_2), 109.3 (C-12), 110.8 (C-2), 112.1 (C-10), 113.4 (C-9), 115.3 (C-6), 126.7 (C- p,p'), 127.3 (C- m,m'), 133.2 (C- o,o'), 138.4 (C-1), 140.0 (C-8), 148.6 (C-11), 152.9 (C-3), 155.9 (C-7), 158.5 (C-13) ppm. ^{11}B NMR (CDCl_3 , 96 MHz) δ : 11.5 ppm. HRMS Calc. m/z for $\text{C}_{29}\text{H}_{29}\text{BN}_3\text{O}_3$ [$\text{M}^+ + \text{H}$] $^+$: 478.2300. Found: 478.2290, error 1.0343 ppm.

2.2.2. **2c**: *N,N*-Diethyl-2,2-diphenyl-3-(3,5-dinitrophenyl)-2H-benzo[e][1,3,2]oxazaborinin-7-amine

The title of compound was prepared from the reaction of ligand **1c** 0.96 g (2.7 mmol) and diphenylborinic acid 0.51 g (2.8 mmol) in ether ethylic as a solvent at reflux temperature for 3 h to give 1.04 g (2.1 mmol, 71% yield). IR (ATR): 3102, 1597, 1528, 1489, 1458, 1431, 1342, 1264, 1217, 1121, 979, 726, 705 cm^{-1} . ^1H NMR (CDCl_3 , 300 MHz) δ : 3.85 (3H, OCH_3), 7.29–7.17 (6H, m, H- m,m',p,p'), 7.41 (4H, d, $J = 6.6$ Hz, H- o,o'), 7.81 (1H, d, $J = 6.9$ Hz, H-5), 8.22 (2H, s, H-9), 8.35 (1H, s, H-11), 8.81 (1H, s, H-7) ppm. ^{13}C NMR (CDCl_3 , 75 MHz) δ : 56.0 (C- OCH_3), 102.0 (C-2), 111.2 (C-4), 117.1 (C-11), 124.7 (C-9), 127.1 (C- p,p'), 127.5 (C- m,m'), 131.4 (C-6), 133.4 (C- o,o'), 134.5 (C-5), 147.2 (C-10), 148.0 (C-8), 161.5 (C-7), 166.8 (C-3), 170.9 (C-1) ppm. ^{11}B NMR (CDCl_3 , 96 MHz) δ : 6.0 ppm. HRMS Calc. m/z for $\text{C}_{26}\text{H}_{21}\text{BN}_3\text{O}_6$ [$\text{M}^+ + \text{H}$] $^+$: 482.1526. Found: 482.1517, error 1.6749 ppm.



Scheme 1. Reaction of ligands **1a–1c** with phenylboronic acid to obtain boron derivatives **2a–2c**.

2.3. Single crystal X-ray structure determinations

Suitable crystals for X-ray diffraction analysis of ligands and boron complexes were grown from saturated methanol, chloroform or dichloromethane solutions at room temperature. Crystal growing up was got for slow evaporation of the solvent (3–4 days). All diffraction data were measured using an Enraf Nonius Kappa-CCD diffractometer with graphite monochromated $\lambda_{\text{Mo K}\alpha} = 0.71073 \text{ \AA}$. Frames were collected at $T = 293 \text{ K}$ via ω/ϕ rotation. Direct methods SIR2004 [29] and SHELXS-86 [30] were used for structure solution and the SHELXL-97 [31] software package for refinement and data output. C–H hydrogen atoms were placed in geometrically calculated position using a riding model.

2.4. THG Maker-Fringe measurements and linear absorption

The nonlinear optical measurements were performed in solid state (solid films) using the guest (molecule)–host (polymer) approach. Mixtures of polystyrene (PS) and compounds **1a–1c** and **2a–2c** 70:30 wt.% ratio, respectively, were dissolved in chloroform. The solid films were deposited on fused silica substrates (1 mm-thick) by using the spin coating technique. The prepared films had typical thickness between 77 and 170 nm with good optical quality. Absorption spectra of the spin-coated films were obtained with a spectrophotometer (Perkin–Elmer Lambda 900). Sample thickness was measured by a Dektak 6M profiler.

THG Maker-Fringes setup is reported elsewhere [32,33]. Briefly, it consisted of a Nd-YAG laser-pumped optical parametric oscillator (OPO) that delivered pulses of 8 ns at a repetition rate of 10 Hz. A fundamental wavelength of 1200 nm (idler beam) was used. The output of the OPO system was focused into the films with a 30-cm focal-length lens to form a spot with a radius of approximately 150 μm . Typical energies in our measurements were set at 1 mJ per pulse at sample position (corresponding to peak intensities of $\sim 0.18 \text{ GW/cm}^2$). The third-harmonic beam, as a bulk effect, emerging from the films was separated from the pump beam by using a color filter and detected with a PMT and a Lock-in amplifier. The THG measurements were performed for incident angles in the range from -40° to 40° with steps of 0.27° . All the experiment was computer-controlled.

In the Maker-Fringes technique, the third-harmonic peak intensity $I^{3\omega}$ from the substrate-film structure is compared to that one produced from the substrate alone. Then, the nonlinear susceptibility $\chi^{(3)}$ in a film of thickness L_f is determined from:

$$\chi^{(3)} = \chi_s^{(3)} \frac{2}{\pi} L_{c,s} \left(\frac{\alpha/2}{1 - \exp(\alpha L_f/2)} \right) \left(\frac{I_f^{3\omega}}{I_s^{3\omega}} \right)^{1/2} \quad (1)$$

where $\chi_s^{(3)}$ and $L_{c,s}$ are the nonlinear susceptibility and coherence length, respectively, for the substrate at the fundamental wavelength, and α is the film absorption coefficient at the harmonic wavelength [34]. In our calculation we considered $\chi_s^{(3)} = 3.1 \times 10^{-14} \text{ esu}$ and $L_{c,s} = 9.0 \mu\text{m}$ for the fused silica substrate [32,33]. Our samples satisfied the condition $L_f \ll L_{c,s}$ in which the Eq. (1) is valid.

3. Results and discussion

3.1. X-ray diffraction analysis

The molecular structures for compounds **1b**, **1c**, and **2a–2c** were confirmed by X-ray diffraction analysis (see Fig. 1 and Table 1). Details for **1a** can be found elsewhere [35]. Compounds **1b–1c**, **2a** and **2c** crystallize in the monoclinic space group $P2_1/c$ containing four and eight (**2c**) molecules per unit cell. Compound **2b** crystallizes in triclinic space group $P\bar{1}$, with one independent molecule in the

unit cell. In general, X-ray analysis of compounds **1b** and **1c** showed a main π -backbone containing two aromatic ring linked by azomethine (HC=N) moiety near to a planar conformation, this feature is also showed for the reported compound **1a**. Compounds **1a–1c** have in their structure the HO–C–C–C=N= or =N–C–C–OH fragment, which were employed for the boron complexation in **2a–2c**, for these compounds a tetrahedral boron atom was confirmed by their X-ray diffraction analysis. The main structural feature after boron complexation in **2a** and **2c** (**2c** has two molecules in the asymmetric unit) is the twisted conformation of the aza- π -backbone as is shown by the torsion angles for the C(7)–N–ph (ph = C(8)–C(9)) fragment, which exhibits values of $43.4(6)^\circ$ and $46.7(4)^\circ$ ($-51.1(4)^\circ$), respectively. In comparison, their corresponding ligands **1a** and **1c** present values of $10.6(4)^\circ$ [35] and $39.0(3)^\circ$, respectively. This bent structure for compounds **2a** and **2c** could be attributed to the steric effect provoked by the two phenyl groups bonded directly to the boron atom (see Section 3 on the next paragraph about boron angles). Furthermore, the bond distances for $\text{C}_{\text{ph}}\text{--C=N--C}_{\text{ph}}$ fragment indicate the electronic changes after boron complexation: the largest variation is over the bond connecting the aromatic ring and the iminic carbon atom $\text{C}_{\text{ph}}\text{--C}$ from compound **2a** ($1.394(7) \text{ \AA}$) and **2c** ($1.406(4) \text{ \AA}$, $1.393(4) \text{ \AA}$) to ligands **1a** ($1.425(3) \text{ \AA}$) and **1c** ($1.439(2) \text{ \AA}$). However, the X-ray diffraction analysis for compound **2b** showed that the formation of five-membered heterocycle after boron complexation conserves the planar conformation in the aza- π -backbone, being the C(7)–N–C(8)–C(9) torsion angle of **1b** ($5.1(4)^\circ$) and **2b** ($1.4(3)^\circ$), (see Table 2). Moreover, the change in the distance for the bond $\text{C}_{\text{ph}}\text{--C}$ is shorter than that for compounds **2a** and **2c**. Previous to get the X-ray data of compound **2a**, a theoretical approximation of this structure was developed using the GAUSSIAN-98 program package [36] within the framework of the density functional theory (DFT) at the B3PW91/6-31G* level. Its metric parameters were taken from the X-ray data of **2c**. The theoretical estimation of the torsion angle for C=N-ph fragment is of 40° , which is close to the experimental value of $43.4(6)^\circ$.

Analyses of angles around the boron atom for compounds **2a–2c** confirm the tetrahedral geometry surrounding this atom; data are shown in Table 3. A detailed analysis confirms that in compounds **2a** and **2c**, the complexation of the boron atom produces a six-membered heterocycle with angles from $105.5(3)^\circ$ to $118.8(3)^\circ$ around this one. In contrast, for compound **2b** the formation of a heterocycle with five members is produced after the complexation reaction and shows angles from $98.90(15)^\circ$ to $118.95(18)^\circ$ around the boron atom. A comparison of the angle O–B–N for boron compounds showed that in compound **2b** ($98.90(15)^\circ$) it is considerably smaller than that of the same fragment in derivative **2a** ($105.7(3)^\circ$) and **2c** ($106.5(2)^\circ$, $104.4(2)^\circ$). This angle change in boron compounds, could give an explanation of the bent structure showed for **2a** and **2c**. Larger angles for O–B–N, $105.7(3)^\circ$ in **2a** and $106.5(2)^\circ$, $104.4(2)^\circ$ in **2c**, close to the two phenyl rings bonded to the boron atom at the main π -backbone, develop a steric effect that promotes a bent structure in such compounds. On the contrary, with a smaller angle, $98.90(15)^\circ$ in **2b**, a flat conformation in the π -backbone is observed. Furthermore, the molecular elongation between the aromatic ring and the boron heterocycle on **2b** reduces the steric effect, in contrast to compounds **2a** and **2c** where a bent conformation is promoted by this fact.

3.2. Optical measurements

Absorption spectra of compounds **1a–1b** and **2a–2b** were obtained in solid thin polymer films (see Fig. 2; spectra for **1c** and **2c** were removed for clarity reasons). In general, for compounds **1a–1c** a $n \rightarrow \pi^*$ electronic transition is the responsible for the main absorption bands, and it could be modified by the conformational

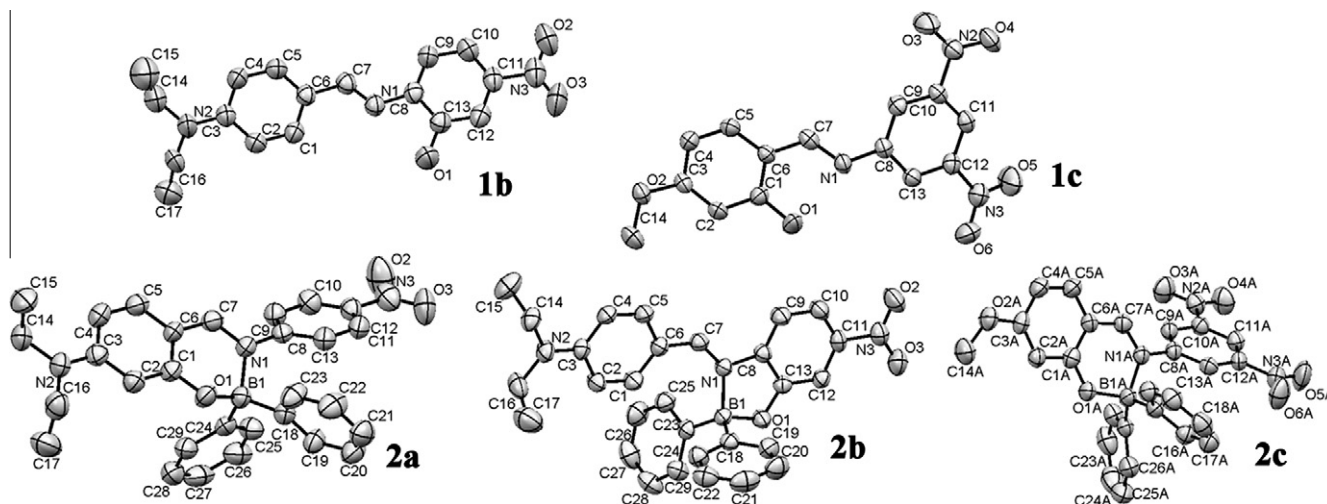


Fig. 1. Crystal structures of compounds **1b**, **1c**, **2a**, **2b**, and **2c**.

Table 1
Selected crystal and refinement data for compounds **1b–1c** and **2a–2c**.

Crystal data ^a	1b	1c	2a	2b	2c
Formula	C ₁₇ H ₁₉ N ₃ O ₃	C ₁₄ H ₁₁ N ₃ O ₆	C ₂₉ H ₂₈ BN ₃ O ₃	C ₂₉ H ₂₈ BN ₃ O ₃	C ₂₆ H ₂₀ BN ₃ O ₆
MW (g/mol)	313.35	317.26	477.35	477.37	481.26
Crystal system	monoclinic	monoclinic	monoclinic	triclinic	monoclinic
Space group	<i>P</i> 2 ₁ / <i>c</i>	<i>P</i> 2 ₁ / <i>c</i>	<i>P</i> 2 ₁ / <i>c</i>	<i>P</i> 1̄	<i>P</i> 2 ₁ / <i>c</i>
<i>a</i> (Å)	16.9980(6)	15.6324(6)	14.617(3)	9.7596(3)	16.3993(7)
<i>b</i> (Å)	7.5664(3)	6.9274(3)	18.471(4)	11.7284(4)	20.2180(12)
<i>c</i> (Å)	13.0501(3)	14.2773(5)	9.824(2)	12.1983(5)	13.7205(6)
α (°)	90	90	90	86.609(2)	90
β (°)	106.811(3)	114.703(3)	107.87(3)	69.189(2)	90.096(2)
γ (°)	90	90	90	72.439(2)	90
<i>V</i> (Å ³)	1606.69(10)	1404.63(10)	2524.9(9)	1242.54(8)	4549.2(4)
<i>Z</i>	4	4	4	2	8
ρ_{calc} (g/cm ³)	1.295	1.500	1.256	1.276	1.405
Collected reflections	9880	7159	6482	7214	21223
Independent reflections	3593	3191	4892	5202	9820
Observed reflections	3593	3191	2425	2571	4961
$R_1 [I > 2\sigma(I)]^b$	0.0763	0.0508	0.0558	0.0591	0.0708
R_w (all data) ^c	0.2226	0.1409	0.0796	0.1429	0.2115
$\Delta\rho_{\text{max}}$ (e Å ⁻³)	0.287	0.178	0.23	0.206	0.0204
$\Delta\rho_{\text{min}}$ (e Å ⁻³)	-0.177	-0.192	-0.175	-0.168	-0.236

^a $\lambda_{\text{MoK}\alpha} = 0.7103$ Å.

^b $R = \sum (F_o^2 - F_c^2) / \sum F_o^2$.

^c $R_w = [\sum w(F_o^2 - F_c^2)^2 / \sum w(F_o^2)^2]^{1/2}$.

Table 2
Structural parameters of the boron complexation in the C=N-ph fragment.

Molecule	C _{ph} -C (Å)	C=N (Å)	N-C _{ph} (Å)	Torsion angle (°) C=N-ph
1a [35]	1.425(4)	1.298(4)	1.407(3)	10.6(4)
2a	1.394(7)	1.312(6)	1.433(6)	43.4(6)
1b	1.439(3)	1.278(3)	1.406(3)	5.1(4)
2b	1.426(3)	1.307(2)	1.415(3)	1.4(3)
1c	1.439(4)	1.289(3)	1.408(2)	39.0(3)
2c ^a	1.393(4)	1.308(4)	1.422(4)	-51.1(4)
	1.406(4)	1.294(4)	1.438(4)	46.7(4)

^a For this crystal structure there are two sets of values arising from the two independent molecules.

planarity of the π -system or by the electronic effect due to the N \rightarrow B coordinative bond on **2a–2c**. In Fig. 2, the absorption band of compound **2a** presented a red shift of 17 nm with respect to its ligand **1a** which is smaller than that observed from **1b** to **2b**: 56 nm. These results are in agreement with the conformational parameters observed in solid state, for compounds **1b** and **2b**, a

Table 3
Angle values (°) around boron atom for compound **2a–2c**.

Angle	2a	2b	2c ^a
O-B-C _{ph1}	105.5(3)	106.94(17)	105.1(3)
			105.7(3)
O-B-C _{ph2}	110.9(3)	108.70(18)	109.3(3)
			109.7(3)
C _{ph2} -B-C _{ph2}	116.8(3)	118.95(18)	118.8(3)
			117.9(3)
O-B-N	105.7(3)	98.90(15)	106.5(2)
			104.4(2)
C _{ph1} -B-N	111.2(3)	113.34(18)	108.3(3)
			108.7(3)
C _{ph2} -B-N	106.2(3)	108.03(16)	108.3(2)
			109.6(3)

^a For this crystal structure there are two sets of values arising from the two independent molecules.

pronounced red shift is related to the contribution of the flat π -backbone (see Section 3.1) and the π -electronic polarization effect due to the N \rightarrow B bond. Whereas, for **1a** and **2a**, the X ray

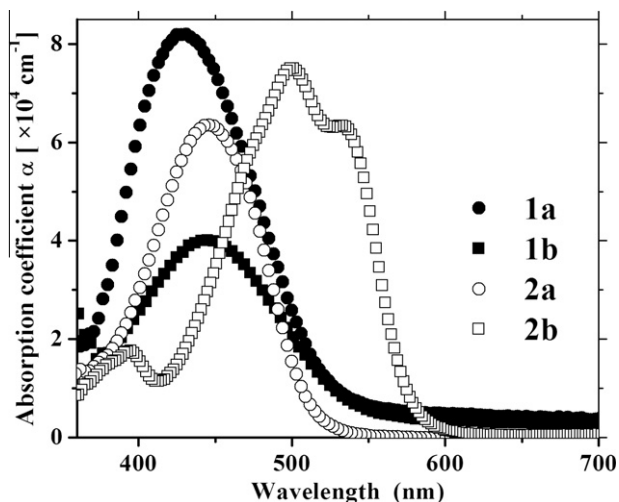


Fig. 2. Absorption spectra for compounds **1a–1b** and **2a–2b** in solid state films doped into polystyrene (PS) at 30:70 wt.%.

diffraction analysis indicates a bent structure, which gives an electronic transition less efficient and so, smaller red shift than that for compound **2b**.

Additionally, cubic nonlinear susceptibilities for the polymer films doped with compounds **1a–1b** and **2a–2b** were evaluated through the THG Maker-Fringes technique [32,33]. For **1c** and **2c**, due to the structural donor– π -acceptor arrangement and strength of the donor group, the THG signal was very weak and below the range of sensitivity for our experimental setup, so the estimation of their $\chi^{(3)}$ values was not possible. The choice of using this technique to measure $\chi^{(3)}$ is because it allowed us to measure pure electronic NLO effects, which is important for high bandwidth photonic applications. As an example of these experiments, Fig. 3 shows the so called THG Maker-Fringe pattern for **1a** film. As reference, the figure also includes the THG pattern measured from the fused silica substrate alone (thickness: 1 mm). These data were obtained at the fundamental near infrared wavelength of 1200 nm (THG signal in 400 nm). From these data is estimated that the third-order nonlinear susceptibility of the **1a** film is on the order of 9.5×10^{-12} esu at such fundamental wavelength. Table 4 summarizes the cubic measurements for the other compounds.

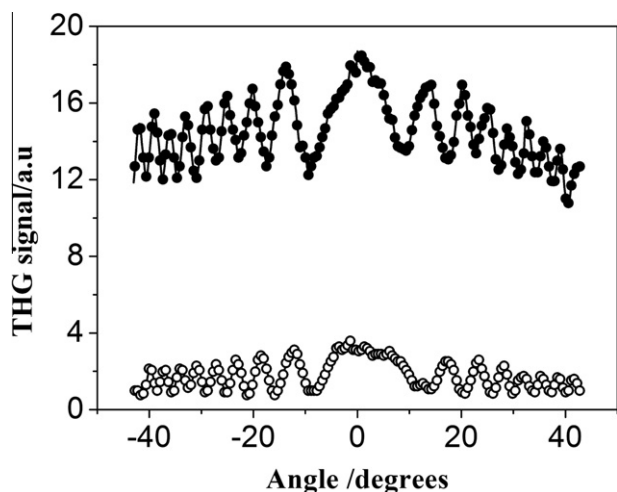


Fig. 3. Third-harmonic light pattern as a function of the incident angle for a thin polymer film (77 nm) (filled circles) doped with 30 wt.% of compound **1a**, and for the 1 mm thick fused silica substrate alone (open circles). The fundamental wavelength is 1200 nm.

Table 4

Maximum absorption coefficient (α), maximum absorption band (λ_{\max}), and cubic susceptibility ($\chi^{(3)}$ at 1200 nm) for ligands **1a–1b** and boronates **2a–2b** into PS (30:70 wt.%), in solid state.

Thin films in PS (30:70 wt.%)	α ($\times 10^4 \text{ cm}^{-1}$)	λ_{\max} (nm)	$\chi^{(3)}$ ($\times 10^{-12}$ esu)
1a	8.2	428	9.5
2a	6.3	445	3.6
1b	4.0	444	5.3
2b	7.5	500	4.1

Notes: 1) For **1c** and **2c** was not possible to measure $\chi^{(3)}$ due to their poor response. 2) $\chi^{(3)}$ for fused silica = 3.1×10^{-14} esu at 1200 nm.

In general, data show that $\chi^{(3)}$ decreases from ligands **1a–1b** to boron complexes **2a–2b**; in the case of **2a** a reduction of $\chi^{(3)}$ by a factor of 2.6 was observed. With respect to the compounds **b**, there was a decrease by just a factor of 1.3 after boron complexation. Since the conformational arrangement of the π -skeleton is modified with the boron complexation (see X-ray analysis for **2a–2c**) then a plausible explanation for the experimental decrease of the cubic susceptibility for **2a** could be that the boron complexation promotes a non-planar conformation in the main aza- π -system

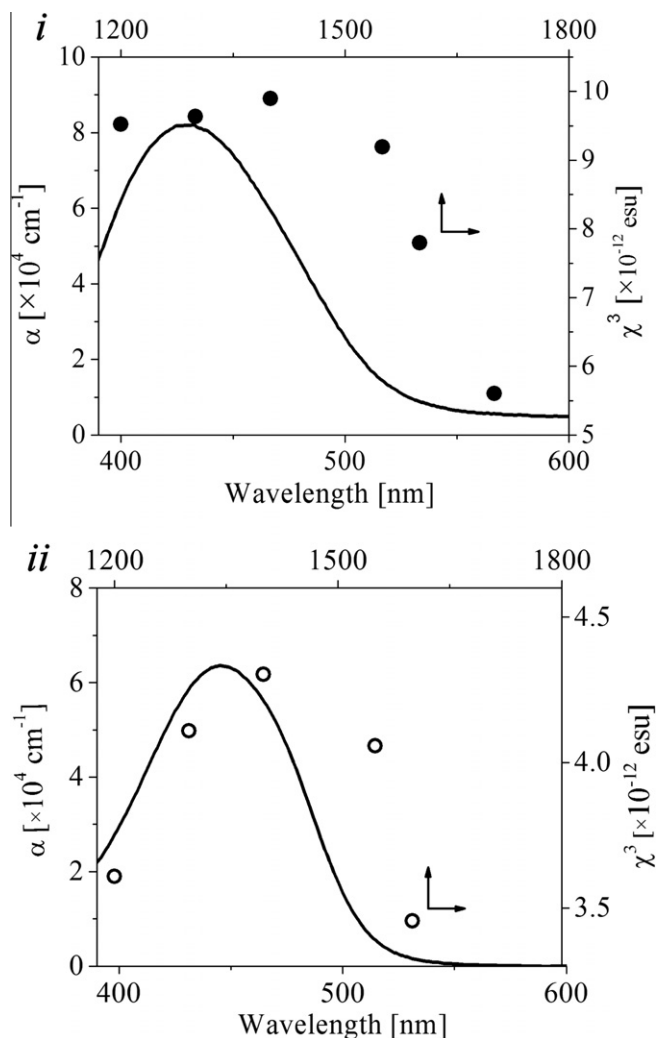


Fig. 4. Wavelength dependence of the $\chi^{(3)}$ susceptibility for a polymer film doped with 30 wt.% of compound **1a** (graph i) and **2a** (graph ii): top and right axes: \bullet and \circ , respectively. As reference, the absorption spectrum for the corresponding films is included (continuous line: bottom and left axes).

as is shown in Fig. 1 and data in Table 2 (torsion angles). In the case of compounds **1b** and **2b**, even when the X-ray data indicate that the planarity is preserved after boron complexation and that the UV spectra show a red shift, not any considerable change is observed for $\chi^{(3)}$ values. The key to explain this observation could be associated with the deformation of the electronic π -system from ligand to boron complex, ligands have a D- π -C=N- π -A arrangement (effective D- π -A push-pull architecture) but the formation of the N \rightarrow B bond produces a D- π -C=N⁺- π -A system, which it also might be viewed as a D- π -A- π -A structure. In this way, the D-A combination presented in compounds **2a–2c** could be less efficient for third-harmonic generation than those for the ligands **1a–1c**.

Note that in the calculation of $\chi^{(3)}$ it is important to consider the absorption of the films according to the formalism of the Maker-Fringes technique (see Eq. (1)). The absorption coefficients (α) at 400 nm for **1a**, **1b**, **2a** and **2b** are 6.2, 2.5, 2.9 and $1.5 \times 10^4 \text{ cm}^{-1}$, respectively, so there is not a significant difference between them in the $\chi^{(3)}$ values through three-photon resonance (about a factor of less than 1.5 times for the largest difference on the cubic susceptibility values) when using the wavelength of 1200 nm (see Eq. (1)).

The wavelength dependence of the third-order nonlinear susceptibility for compounds **1a** and **2a** was also determined (see Fig. 4). To clarify this multi-photon resonance, Fig. 4 includes the linear absorption spectrum of the film (bottom and left axes). Note that the wavelength scales are arranged in such a way that the top scale is 3 times the bottom one. Thus, according to the absorption peaks located at 428 and 445 nm for **1a** and **2a**, respectively, there is a slight enhancement of the cubic nonlinearities through three-photon resonances, which is more notorious for **1a** compound than for **2a**.

4. Conclusions

We have synthesized three borinates **2a–2c** and their chemical structures were established by NMR data; information of compound **2a** was compared with data lately reported. Third-order nonlinear susceptibilities were measured at IR wavelengths for compounds **1a–1b** and **2a–2b**. Reduction on the cubic susceptibility from **1a–1b** to **2a–2b** (for family **c** was not possible to measure $\chi^{(3)}$ because of the poor THG response) was related to structural features. Structurally, compound **2a** showed a larger twisted conformation with respect to its ligand **1a**, which was estimated by computed calculations using the density functional theory (DFT) at the B3PW91/6-31G* level and confirmed by X-ray diffraction analysis. In the case of compound **2b**, a smaller reduction of $\chi^{(3)}$ with respect to that one for **2a**, was estimated when going from ligands **1b** (reduction of 1.3) and **1a** (reduction of 2.6), respectively; it might be just to the deformation of the electronic π system (from D- π -A to D- π -A- π -A after boron complexation in **2b**) because the X-ray data indicate that its planarity is preserved. In the wavelength dependence of $\chi^{(3)}$, a slight enhancement through three-photon resonances was also observed. These π -backbones like systems, as interesting dyes with structural and electronic features that affect their NLO properties, could have different interesting optical properties, such as Two Photon Absorption (TPA), particularly, through their re-design with appropriate combination of the electronic groups.

Acknowledgements

M. Rodríguez thanks Postdoctoral CONACyT Grant. This work was supported by CONACyT projects 55250, 49512, 58783, 83519; CONACyT-SENER 153094 and PAPIIT IN-214010. Authors

thank M. Olmos, M.A Leyva and Dr. R. Espinosa-Luna for their technical assistance.

Appendix A. Supplementary data

CCDC 865882, 865883, 865884, 865885 and 865881 contains the supplementary crystallographic data for **1b**, **1c**, **2a**, **2b** and **2c**. These data can be obtained free of charge via <http://www.ccdc.cam.ac.uk/conts/retrieving.html>, or from the Cambridge Crystallographic Data Centre, 12 Union Road, Cambridge CB2 1EZ, UK; fax: (+44) 1223-336-033; or e-mail: deposit@ccdc.cam.ac.uk.

References

- [1] N. Fujita, S. Shinkai, T.D. James, *Chem. Asian J.* 3 (2008) 1076.
- [2] K. Gießler, H. Griesser, D. Göhringer, T. Sabirov, C. Richert, *Eur. J. Org. Chem.* 2010 (2010) 3611.
- [3] A.E. Hargrove, R.N. Reyes, I. Riddington, E.V. Anslyn, J.L. Sessler, *Org. Lett.* 12 (2010) 4804.
- [4] Y.L. Rao, S. Wang, *Inorg. Chem.* 50 (2011) 12263.
- [5] J.L. Maldonado, G. Ramos-Ortíz, O. Barbosa-García, M.A. Meneses-Nava, L. Márquez, M. Olmos-López, H. Reyes, B. Muñoz, N. Farfán, *Int. J. Mod. Phys. B* 21 (2007) 2625.
- [6] S. Schlecht, W. Frank, M. Braund, *Eur. J. Org. Chem.* 2010 (2010) 3721.
- [7] H. Höpfl, *J. Organomet. Chem.* 581 (1999) 129.
- [8] Y. Qin, I. Kibur, S. Shah, F. Jäkle, *Org. Lett.* 8 (2006) 5227.
- [9] D. Frath, S. Azizi, G. Uldrich, P. Retailleau, R. Ziessel, *Org. Lett.* 13 (2011) 3414.
- [10] S.P. Forrest, M.K. Thompson, *Chem. Rev.* 107 (2007) 923.
- [11] S.R. Marder, *J. Mater. Chem.* 19 (2009) 7392.
- [12] C. Fuentes-Hernández, G. Ramos-Ortíz, S.Y. Tseng, M.P. Gaj, B. Kippelen, *J. Mater. Chem.* 19 (2009) 7394.
- [13] G. Ramos-Ortíz, J.L. Maldonado, M.C.G. Hernández, M.G. Zolotukhin, S. Fomine, N. Fröhlich, U. Scherf, F. Galbrech, E. Preis, M. Salmon, J. Cárdenas, M.I. Chávez, *Polymer* 51 (2010) 2351.
- [14] J.P. Morrall, G.T. Dalton, M.G. Humphrey, M. Samoc, *Adv. Organomet. Chem.* 51 (2008) 61.
- [15] B.J. Coe, J.A. Harris, J.J. Hall, B.S. Brunshwing, S.T. Hung, W. Libaers, K. Clays, S.J. Coles, P.N. Horton, M.E. Light, M.B. Hursthouse, J. Garín, *J. Org. Chem. Mater.* 18 (2006) 5907.
- [16] H.S. Nalwa, S. Miyata (Eds.), *Nonlinear Optics of Organic Molecules and Polymers*, CRC Press, Boca Raton FL, 1997.
- [17] E.E. Moore, D. Yaron, *J. Phys. Chem. A* 106 (2002) 5339.
- [18] S.R. Marder, J.W. Perry, G. Bourhill, C.B. Gorman, B.G. Tiemann, K. Mansour, *Science* 261 (1993) 186.
- [19] B.M. Muñoz, R. Santillan, M. Rodríguez, J.M. Méndez, M. Romero, N. Farfán, P.G. Lacroix, K. Nakatani, G. Ramos-Ortíz, J.L. Maldonado, *J. Organomet. Chem.* 693 (2008) 1321.
- [20] M. Rodríguez, R. Castro-Beltrán, G. Ramos-Ortíz, J.L. Maldonado, N. Farfán, O. Domínguez, J. Rodríguez, R. Santillan, M.A. Meneses-Nava, O. Barbosa-García, J. Peón, *Synth. Met.* 159 (2009) 1281.
- [21] M. Rodríguez, J.L. Maldonado, G. Ramos-Ortíz, J.F. Lamère, P. Lacroix, N. Farfán, M.E. Ochoa, R. Santillan, M.A. Meneses-Nava, O. Barbosa-García, K. Nakatani, *New J. Chem.* 33 (2009) 1693.
- [22] J.F. Lamère, P.G. Lacroix, N. Farfán, J.M. Rivera, R. Santillan, K. Nakatani, *J. Mater. Chem.* 16 (2006) 2913.
- [23] J.L. Maldonado, Y. Ponce-de-León, G. Ramos-Ortíz, M. Rodríguez, M.A. Meneses-Nava, O. Barbosa-García, R. Santillan, N. Farfán, *J. Phys. D* 42 (2009) 075102.
- [24] V.M. Herrera-Ambriz, J.L. Maldonado, M. Rodríguez, R. Castro-Beltrán, G. Ramos-Ortíz, N.E. Magaña-Vergara, M.A. Meneses-Nava, O. Barbosa-García, R. Santillan, N. Farfán, F.X. Dang, P.G. Lacroix, I. Ledoux-Rak, *J. Phys. Chem. C* 115 (2011) 23955.
- [25] F. Qiao, A. Liu, Y. Zhou, Y. Xiao, P.O. Yang, *J. Mater. Sci.* 44 (2009) 1283.
- [26] J.F. Salinas, J.L. Maldonado, G. Ramos-Ortíz, M. Rodríguez, M.A. Meneses-Nava, O. Barbosa-García, R. Santillan, N. Farfán, *Sol. Energy Mater. Sol. Cells* 95 (2011) 595.
- [27] J.W. Ledbetter, *J. Phys. Chem.* 72 (1968) 4111.
- [28] G. Chremos, H. Weidmann, H. Zimmerman, *J. Org. Chem.* 26 (1961) 1683.
- [29] M.C. Burla, R. Caliandro, M. Camalli, B. Carrozzini, G.L. Cascarano, L. De Caro, C. Giacovazzo, G. Polidori, R. Spagna, *J. Appl. Crystallogr.* 38 (2005) 381.
- [30] G.M. Sheldrick, *SHELXS-86* – Program for Crystal Structure Solution, University of Göttingen, Germany, 1986.
- [31] G.M. Sheldrick, *SHELXL-97* – Program for the Refinement of Crystal Structure, University of Göttingen, Germany, 1997.
- [32] G. Ramos-Ortíz, J.L. Maldonado, M.A. Meneses-Nava, O. Barbosa-García, M. Olmos-López, M. Cha, *Opt. Mater.* 29 (2007) 636.
- [33] E. Klimova, T. Klimova, J.M. Martínez-Mendoza, L. Ortíz-Frade, J.L. Maldonado, G. Ramos-Ortíz, M. Flores-Alamo, M. Martínez-García, *Inorg. Chim. Acta* 362 (2009) 2820.
- [34] X.H. Wang, D.P. West, N.B. McKeown, T.A. King, *J. Opt. Soc. Am. B* 15 (1998) 1895.

- [35] P.G. Lacroix, F. Averseng, I. Malfant, K. Nakatani, *Inorg. Chim. Acta* 357 (2004) 3825.
- [36] M.J. Frisch, G.W. Trucks, H.B. Schlegel, G.E. Scuseria, M.A. Robb, J.R. Cheeseman, V.G. Zakrzewski, J.A. Montgomery, Jr., R.E. Stratmann, J.C. Burant, S. Dapprich, J.M. Millam, A.D. Daniels, K.N. Kudin, M.C. Strain, O. Farkas, J. Tomasi, V. Barone, M. Cossi, R. Cammi, B. Mennucci, C. Pomelli, C. Adamo, S. Clifford, J. Ochterski, G.A. Petersson, P.Y. Ayala, Q. Cui, K. Morokuma, D.K. Malick, A.D. Rabuck, K. Raghavachari, J.B. Foresman, J. Cioslowski, J.V. Ortiz, A.G. Baboul, B.B. Stefanov, G. Liu, A. Liashenko, P. Piskorz, I. Komaromi, R. Gomperts, R.L. Martin, D.J. Fox, T. Keith, M.A. Al-Laham, C.Y. Peng, A. Nanayakkara, C. Gonzalez, M. Challacombe, P.M. W. Gill, B. Johnson, W. Chen, M.W. Wong, J.L. Andres, C. González, M. Head-Gordon, E.S. Replogle, J.A. Pople, *Gaussian 98 (Revision A.9)*, Gaussian, Inc., Pittsburgh, PA, 1998.